

pubs.acs.org/acscatalysis Research Article

# Structural and Substrate Specificity Analysis of 3-O-Sulfotransferase Isoform 5 to Synthesize Heparan Sulfate

Rylee Wander, Andrea M. Kaminski, Zhangjie Wang, Eduardo Stancanelli, Yongmei Xu, Vijayakanth Pagadala, Jine Li, Juno M. Krahn, Truong Quang Pham, Jian Liu,\* and Lars C. Pedersen



ABSTRACT: Heparan sulfate 3-O-sulfotransferase (3-OST) transfers a sulfo group to the 3-OH position of a glucosamine saccharide unit to form 3-O-sulfated heparan sulfate. 3-O-sulfation is known to be critically important for bestowing anticoagulant activity and other biological functions of heparan sulfate. Here, we report two ternary crystal structures of 3-OST isoform 5 (3-OST-5) with 3'-phosphoadenosine-5'-phosphate (PAP) and two octasaccharide substrates. We also used 3-OST-5 to synthesize six 3-O-sulfated 8-mers. Results from the structural analysis of the six 3-O-sulfated 8-mers revealed the substrate specificity of 3-OST-5. The enzyme prefers to sulfate a 6-O-sulfo glucosamine saccharide that is surrounded by glucuronic acid over a 6-O-sulfo glucosamine saccharide that is surrounded by 2-O-sulfated iduronic acid. 3-OST-5-modified 8-mers display a broad range of anti-factor Xa activity, depending on the structure of the 8-mer. We also discovered that the substrate specificity of 3-OST-5 is not governed solely by the side chains from amino acid residues in the active site. The conformational flexibility of the 2-O-sulfated iduronic acid in the saccharide substrates also contributes to the substrate specificity. These findings advance our understanding of how to control the biosynthesis of 3-O-sulfated heparan sulfate with the desired biological activities.

KEYWORDS: sulfotransferase, heparan sulfate biosynthesis, chemoenzymatic synthesis, oligosaccharide, protein/substrate complex

eparan sulfates (HSs) are sulfated polysaccharides that are widely present on the surface of mammalian cells and in the extracellular matrix. HS plays a wide range of biological functions, including regulating embryonic development, modulating inflammatory responses, and regulating blood coagulation.1 Heparin, a highly sulfated form of HS, is a commonly used drug to treat blood clotting disorders.<sup>2</sup> Additionally, many viruses utilize cell surface HS on host cells as a receptor to establish infection. Notably, HS is reportedly involved in the infection of SARS-Cov-2.3 HS consists of repeating disaccharide units of either glucuronic acid (GlcA) or iduronic acid (IdoA) linked to a glucosamine (GlcN) saccharide and each saccharide unit can be sulfated. Common sulfations in HSs are found at the N-position and 6-OH positions of GlcN saccharide units as well as the 2-OH position of IdoA saccharide unit. Sulfations of the 3-OH position of GlcN and 2-OH position of GlcA also exist in HS, but are exceedingly rare. The sulfation patterns, the position of both GlcA and IdoA saccharides, and the length of the saccharide chain contribute to the binding affinity of proteins and determine HS's selectivity, regulating biological functions.<sup>4</sup> A central goal in HS-related biological research is to identify the link between the sulfation patterns and biological functions.

A group of specialized enzymes, including glycosyltransferase, C<sub>5</sub>-epimerase, and a series of sulfotransferases participate in the biosynthesis of HS. The concerted actions of these enzymes control the saccharide sequences and quantity of HS. The synthesis of the backbone, composed of a repeating disaccharide sequence of N-acetyl GlcN (GlcNAc) and GlcA is accomplished by glycosyltransferases referred to as HS polymerases. The backbone can be further modified by Ndeacetylase-N-sulfotransferase, converting a GlcNAc to a Nsulfo GlcN (GlcNS) unit. Subsequently,  $C_5$ -epimerase converts the adjacent GlcA to an IdoA unit. The installation of additional sulfo groups is achieved by a 2-O-sulfotransferase, 6-O-sulfotransferases (three isoforms), and 3-O-sulfotransferases (3-OSTs, with seven isoforms). These enzymes act on the backbone in a stepwise manner, generating an extremely diverse set of heparin and HS molecules with diverse length and modification patterns. Because the process is not template-

Revised: September 30, 2021 Revised: November 17, 2021 Published: November 30, 2021





**Figure 1.** Substrate specificity of different 3-OST isoforms. Panel (A) shows the substrate specificity of 3-OST-1. (B) Substrate specificity of 3-OST-3. The IdoA2S saccharide unit near the acceptor site is in  ${}^{2}S_{0}$  skew boat confirmation based on the crystal structure. (C) Substrate specificity of 3-OST-5. The 3-O-sulfation site is circled.

driven, product structures vary substantially and are primarily regulated by the enzyme tissue expression pattern and individual enzyme specificity. Recently, the HS biosynthetic enzymes have been used to synthesize structurally homogeneous HS oligosaccharides. High regioselectivity displayed by HS biosynthetic enzymes has eliminated the need for protection and deprotection steps used in chemical synthesis. As a result, enzyme-based synthesis has dramatically increased the synthesis efficiency, making it a promising alternative approach to synthesize structurally homogeneous oligosaccharides.<sup>6,7</sup> The availability of structurally defined oligosaccharides accelerates efforts to study the relationship between the structure and function of HS and the development of HSbased therapeutics. 8,9 One example is the synthesis of anticoagulant dodecasaccharides to replace animal-sourced low-molecular-weight heparin. 7,9 Synthetic heparin reduces side effects and improves the safety of the supply chain for heparin and low-molecular-weight heparin drugs. The 3-OST isoform 5 (3-OST-5) is a key enzyme used in the process of preparing the anticoagulant dodecasaccharides.<sup>7</sup>

3-OST transfers a sulfo group to the 3-OH position of GlcNS. Although it is a rare modification in HS, the 3-O-sulfation is closely related to the biological functions of HS. Intriguingly, despite the scarcity of 3-O-sulfation in HS, 3-OSTs represent the largest family of HS sulfotransferase, with seven isoforms in the human genome. The isoforms recognize a saccharide sequence around the modification site, generating 3-O-sulfated HS products with distinct biological functions (Figure 1). Based on the current dogma in the field, 3-OST-1 sulfates a GlcNS6S saccharide that is linked to a GlcA on the nonreducing end, conferring anticoagulant activity to HS and heparin. However, 3-OST-3 sulfates a GlcNS that has no 6-O-sulfation and is linked to an IdoA2S saccharide at the nonreducing end of the acceptor

GlcNS. HS modified by 3-OST-3 is an entry receptor for herpes simplex virus-1 (HSV-1). <sup>11</sup> 3-OST-5 is an enzyme that appears to sulfate a GlcNS6S saccharide that is linked to either an IdoA2S or a GlcA on the nonreducing end. In a recent study, the substrate specificity of 3-OST-4 was explored, showing that it also sulfates a GlcNS saccharide that has no 6-O-sulfation. <sup>12</sup> 3-O-sulfated HSs have been reported to regulate axon guidance and growth of neurons, control the progenitor cell expansion for salivary gland development, and were found in high quantities in human granulosa cells, suggesting an importance in ovulation. <sup>13-15</sup> Additionally, different 3-OST isoforms have been implicated in diseases including Alzheimer's disease and cancers. <sup>16-18</sup> The unique substrate specificity of 3-OST isoforms and the potential biological functions of HS modified by different 3-OSTs have attracted interest in understanding the mechanism used by different isoforms to distinguish among saccharide sequences.

In this manuscript, we used structurally homogeneous 8-mer substrates to investigate the substrate specificity of 3-OST-5. The crystal structures of the ternary complexes of 3-OST-5 with 3'-phosphoadenosine-5'-phosphate (PAP) and two different octasaccharide substrates reveal the key amino acid residues involved in interactions with the saccharide substrates at the resolution of 2.90 and 2.75 Å, respectively. Results from the structural analysis of 3-OST-5-modified 8-mers indicate that 3-OST-5 prefers to sulfate a GlcNS6S saccharide that is surrounded by glucuronic acid over one that is surrounded by 2-O-sulfated iduronic acid. 3-OST-5 can generate 8-mers both with and without anticoagulant activity, depending on the saccharide sequences around the 3-O-sulfation site. Compared with previously published structures of 3-OST-1 and 3-OST-3,  $^{19-21}$  we discovered that 3-OST-5 has a very similar structure in the active site and overall structure to 3-OST-1 and 3-OST-3. We also determined that the substrate specificity of 3-OST-5

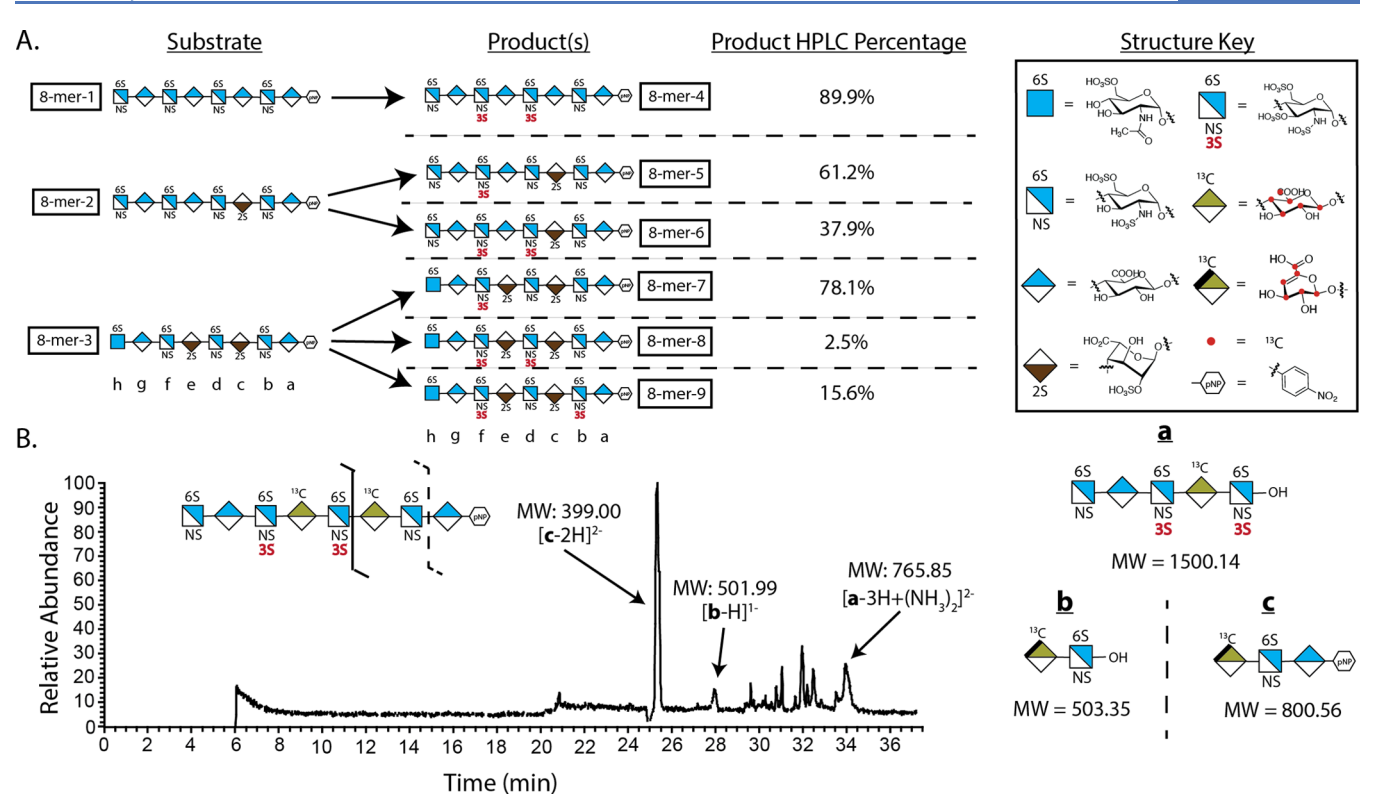


**Figure 2.** Determination of the substrate specificity of 3-OST-5 using 8-mer substrates. (A) Sulfation reaction carried out by 3-OST-5 using 8-mer-1, 8-mer-2, and 8-mer-3 substrates. The structures of the 8-mers are presented in shorthand symbols. The key for the shorthand symbols is presented (right). Red dots in the structures represent sites with <sup>13</sup>C-carbon. (B) Structural analysis of <sup>13</sup>C-labeled 8-mer-4 using the LC-MS/MS method. The schematic digestion of 8-mer by heparin lyases is presented (top). The digested fragments (a-c, diagrammed on the right) were then assessed by liquid chromatography-tandem mass spectrometry (LC-MS/MS). Spectrum analysis allowed for matching the product to a particular structure based on observed mass peaks.

is not only governed by the side chains from amino acid residues in the active site but also by uronic acids flanking both sides of the acceptor. These findings advance our understanding of the regulatory mechanisms controlling the biosynthesis of 3-O-sulfated HS with desired biological activities. The results also expand the capability of synthesizing 3-O-sulfated oligosaccharides using the chemoenzymatic approach.

## RESULTS

3-OST-5 Requires 6-O-Sulfation to Act on a Substrate. Six octasaccharides (8-mers) were synthesized using the chemoenzymatic approach to evaluate the substrate specificity of 3-OST-5 (Supporting Information Figure S1A). The purities of 8-mers were confirmed by high-performance liquid chromatography (HPLC), and molecular masses were verified by electrospray ionization mass spectrometry (ESI-MS) (Supporting Information Figures S2-S7). The substrates used varied in 6-O-sulfation and IdoA2S content. 3-OST-5 was assessed for activity against all substrates using a 35S-labeled sulfo donor, [35S]PAPS (3'-phosphoadenosine-5'-phosphosulfate). The results clearly show that the enzyme was more active toward octasaccharides containing 6-O-sulfation (8-mer-1, -2, and -3) than those without (8-mer-1a, -2a, and -3a) (Supporting Information Figure S1B). Additionally, 3-OST-5 had the highest activity toward the GlcA-only substrate (8mer-1) and the lowest activity toward the substrate containing two IdoA2S residues (8-mer-3). However, there were multiple potential sites for sulfation by 3-OST-5 on each 8-mer

substrate. Using radioactivity alone limited our ability to locate the 3-O-sulfation site. To further assess sites of 3-OST-5 modification, nonradioactive studies were employed.

Determination of the 3-O-Sulfation Sites on 8-mers after 3-OST-5 Modification. To determine the preferred sites for 3-OST-5 sulfation, we incubated 3-OST-5 enzyme with 8-mer-1, -2, and -3 along with PAPS to yield more than six 3-O-sulfated 8-mer products in 0.5-10 mg quantities (Figure 2A). The 3-O-sulfated 8-mers were then subjected to structural determination for the number and location of 3-Osulfo groups. Two subgroups of 3-O-sulfated 8-mers were obtained based on molecular weight measurements (Supporting Information Table S1). One group contained mono-3-Osulfated 8-mers, i.e., 8-mer-5 and 8-mer-7. Another group contained di-3-O-sulfated 8-mers, including 8-mer-4, 8-mer-6, 8-mer-8, and 8-mer-9. Structural analyses of the 3-O-sulfated 8mer products, including 8-mer-4, -5, -6, and -9, were completed using an liquid chromatography-mass spectrometry (LC-MS)/MS-based disaccharide/oligosaccharide analysis<sup>7</sup> (Figure 3, Supporting Information Figures S10–S20). An example to prove the sites of 3-O-sulfation in 8-mer-4 is shown in Figure 2B. Characterization of 8-mer-4 was uniquely challenging using unlabeled 8-mer-1 substrate because it contained three repeated disaccharides of -GlcNS6S-GlcA-, with only two of the repeats carrying a 3-O-sulfo group. To differentiate the repeating disaccharide unit, a site-specific <sup>13</sup>Clabeled 8-mer-1 was synthesized with both saccharides c and e in 8-mer-1 occupied by <sup>13</sup>C-labeled GlcA residues (Supporting Information Figure S8). The corresponding <sup>13</sup>C-labeled 8-mer-

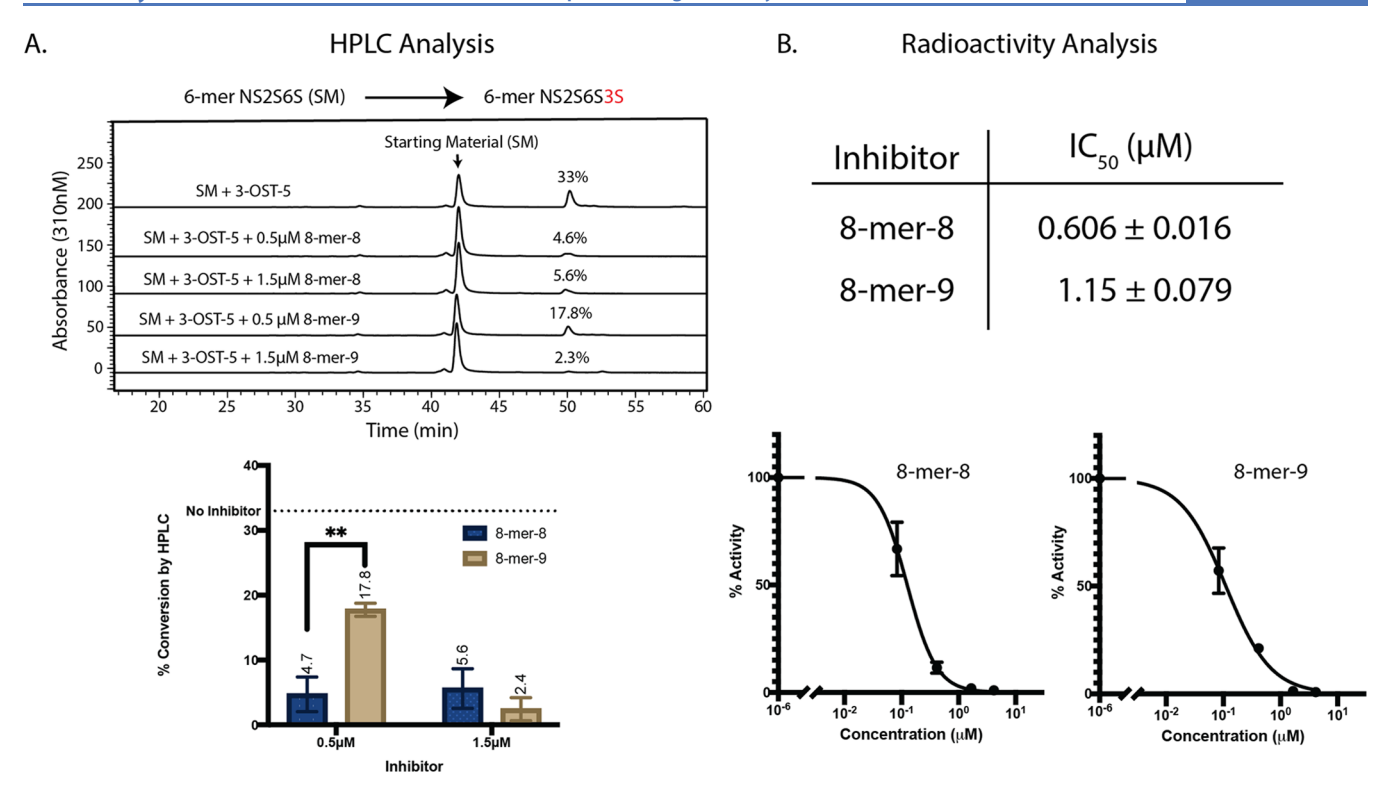


Figure 3. 3-OST-5 is inhibited by 3-O-sulfated 8-mer. (A) HPLC chromatograms of NS2S6S 6-mer modified by 3-OST-3 with or without spiked 8-mer-8 or 8-mer-9. Here, the NS2S6S 6-mer substrate has a saccharide sequence of GlcNS6S-GlcA-GlcNS6S-GlcA-glcNS6S-GlcA-pNP. After 3-OST-5 modification, the 6-mer was transformed to NS2S6S3S 6-mer with a sequence of GlcNS6S-GlcA-GlcNS6S-GlcA-gNP. (B)  $IC_{50}$  values for 8-mer-8 and -9 were then determined in an  $^{35}$ S radioactivity assay. Inhibition curves from 8-mer-8 and -9 are presented. The NS2S6S 6-mer was also used as a substrate in the assay.

4 was generated by incubating 3-OST-5 and the 8-mer-1 (Supporting Information Figure S9). Digestion of the <sup>13</sup>C-labeled 8-mer-4 by heparin lyases resulted in three fragments, a (pentasaccharide), b (disaccharide), and c (trisaccharide), based on the substrate specificity of heparin lyases. <sup>22,23</sup> All three fragments were found from the LC-MS/MS analysis, confirming the locations of 3-O-sulfations on saccharides d and f (Figure 2B). The 3-O-sulfation positions on 8-mer-4 were further confirmed by two-dimensional (2D) NMR (Supporting Information Figures S11 and S12). The structures of 8-mer-7 and -8 were verified by co-elution with 8-mer standards synthesized in previous studies<sup>7,24</sup> (Supporting Information Figures S18 and S19).

Knowing the structures of 3-O-sulfated 8-mer products, we observed trends in substrate preference for 3-OST-5 (Figure 2A). First, in the absence of IdoA2S residues (8-mer-1), 3-OST-5 was highly efficient at installing multiple 3-O-sulfations, generating the di-3-O-sulfated product 8-mer-4 (89.9%) (Figure 2A). The enzyme was less efficient at forming di-3-O-sulfated products with 8-mer-2 and -3 substrates, which contain one and two IdoA2S saccharides, respectively. Using 8mer-2 substrate, 3-OST-5 generated 8-mer-5, a mono-3-Osulfated product, as the major product (61.2%), and 8-mer-6, a di-3-O-sulfated product, was a minor product (37.9%) (Figure 2A). Additionally, when given the choice of modifying saccharide f or saccharide d in 8-mer-2, the enzyme chose to sulfate saccharide f to form trisaccharide domain of -GlcA-GlcNS3S6S-GlcA-. The data suggest that 3-OST-5 preferred the glucosamine site surrounded by GlcA saccharides, not by IdoA2S units (Figure 2A). Lastly, when a substrate contained two IdoA2S saccharides (8-mer-3), 3-OST-5 was able to install

a second 3-O-sulfation on either saccharide b or saccharide d. However, the enzyme preferred to introduce the second 3-O-sulfo group on saccharide b to generate 8-mer-9, where the two 3-O-sulfated glucosamine saccharides are gapped (Figure 2A). It should be noted that the incubation of the reaction mixtures with additional enzymes would lead to increased product formation. However, the identity of products formed as well as the modification site preference (i.e., 8-mer-9 site over 8-mer-8 site) remain consistent.

Product Inhibition of 3-OST-5 by 8-mer-8 and 8-mer-9. We next attempted to explain why 3-OST-5 displayed a preference for producing 8-mer-9 over 8-mer-8. One hypothesis was that the 3-OST-5 enzyme is more susceptible to product inhibition by 8-mer-8 than that by 8-mer-9. The structural difference between 8-mer-8 and 8-mer-9 is the spacing of the 3-O-sulfo groups. In 8-mer-8, the two 3-O-sulfo groups are located on two consecutive glucosamine saccharides, whereas in 8-mer-9, the two 3-O-sulfo groups are located on two glucosamine saccharides that are gapped by a glucosamine. To test the assertion of product inhibition, 3-OST-5 products, 8-mer-8 and 8-mer-9, were first spiked into enzymatic reactions at 0.5 and 1.5  $\mu$ M, respectively (Figure 3). A 6-mer was utilized as the substrate for these reactions to avoid the generation of an additional 8-mer product inhibitor. The products were analyzed by HPLC. Compared to the control, the presence of 8-mer-8 (at the concentration of 0.5  $\mu$ M) reduced product generation 7.0-fold, while a 1.9-fold reduction was observed by 8-mer-9 at the same concentration (Figure 3A). The data suggest that 8-mer-8 displays a stronger inhibition of the activity of 3-OST-5. To further assess the effect of product inhibition on 3-OST-5 activity, IC<sub>50</sub> values for

Table 1. Data Collection and Refinement Statistics

	Trx-3OST5 (I299E)/PAP/8-mer-1 <sup>a,b</sup>	Trx-3OST5 (I299E)/PAP/8mer-2 <sup>a,b</sup>
PDB ID code	7SCD	7SCE
data collection		
space group	$P2_{1}2_{1}2_{1}$	$P2_12_12_1$
cell dimensions		
a, b, c (Å)	55.84, 58.82, 153.11	54.42, 59.00, 151.05
$\alpha$ , $\beta$ , $\gamma$ (deg)	90, 90, 90	90, 90, 90
resolution (Å)	$50.00-2.90 (2.95-2.90)^c$	50-2.75 (2.80-2.75)
$R_{\text{sym}}$ (%)	11.7 (54.7)	16.3 (67.1)
$I/\sigma I$	5.46 (0.86)	7.46 (1.54)
completeness (%)	90.1 (81.3)	99.1 (98.6)
redundancy	3.2 (3.1)	4.9 (4.6)
refinement		
resolution (Å)	$40.50 (2.90)^d$	40.00-2.75
no. of reflections	9311	13196
$R_{\text{work}}/R_{\text{free}}$ (%)	20.82/25.24	18.79/24.60
no. of atoms		
protein	2872	2883
PAP	27	27
oligosaccharide	94	97
water	8	53
B-factors (Å <sup>2</sup> )		
protein	50.87	30.72
PAP	29.05	17.50
oligosaccharide	68.86	55.02
water	18.71	23.95
rms deviations		
bond lengths (Å)	0.006	0.004
bond angles (deg)	1.138	0.761

"A single crystal was used to collect each data set. "These crystals were collected on the Southeast Regional Collaborative Access Team (SER-CAT) 22-ID beamline at the Advanced Photon Source at Argonne National Laboratory. "Values in parentheses are for the highest-resolution shell." The data for the 8mer-1 ternary complex were severely anisotropic and were therefore processed with ellipsoidal truncation by the Diffraction Anisotropy Server (http://www.services.mbi.ucla.edu/anisoscale).

8-mers 8 and 9 were determined using a radioactivity assay, and the same 6-mer substrate was used in the HPLC assay. The data from the inhibition study using <sup>35</sup>S radioactivity were consistent with the HPLC results, with 8-mer-8 as a more potent inhibitor than 8-mer-9 (Figure 3B). The difference in the degree of product inhibition from 8-mer-8 and 8-mer-9 was small but detectable by both radioactive and nonradioactive assays. The data suggest that product inhibition could serve as a contributing factor for 3-OST-5 to preferentially generate 8-mer-9, rather than 8-mer-8.

Crystal Structures of 3-OST-5/PAP/8-mer-1 and 3-OST-5/PAP/8-mer-2. Diffraction quality ternary complex crystals were obtained utilizing a thioredoxin fusion of 3-OST-5 in the presence of PAP and either 8-mer-1 or 8-mer-2. The structures of the complexes with 8-mer-1 and 8-mer-2 were refined to 2.9 and 2.75 Å, respectively (Table 1). A superposition of the 3-OST-5 structures shows a high degree of similarity [root-mean-square deviation (RMSD) 0.333 Å over 260 C $\alpha$  atoms] (Figure 4A). The addition of the *N*-terminal thioredoxin crystallization tag has negligible impact on the overall structure of 3-OST-5 as 3-OST-5 superimposes with an RMSD of 0.597 Å over 258 C $\alpha$  atoms, with the previous crystal structure of 3-OST-5 solved only in the presence of PAP without saccharide substrate and without a thioredoxin tag (Figure 4A).<sup>25</sup> The binding of substrates 8-mer-1 and 8mer-2 to the substrate channel appears to induce small movements in two loops as well as small variations in side

chain rotomers (Figure 4A). The loop (Ala119-Phe125) containing the proposed catalytic base Glu122 has moved into the cleft upon binding to saccharide substrate with the largest shift of up to 2 Å at Ser120. Another loop (Phe297-Lys303) found at the nonreducing end of the binding cleft also appears to have moved into the cleft up to  $\sim 1.5-2$  Å. Four residues on a loop overlying the PAP site that were disordered in the absence of 8-mer substrates (Gly307-Gly310) become ordered upon binding the substrate, forming interactions with both 8-mers via the side chain of Ser308, and with the 3'phosphate of PAP through the backbone amide of Gly310 (Figure 4A,B). Lys309, conserved in 3-OST-1 and 3-OST-3, forms interactions with both the substrate and the 5'phosphate of PAP and is in position to interact with the sulfo group of PAPS (Figure 4A). Mutations of the equivalent lysine in 3-OST-1 to alanine yielded 17% of wt activity while abolishing activity for 3-OST-3, suggesting an important role in the substrate binding and potentially catalysis.<sup>20,3</sup>

Despite the presence of an IdoA2S in the 8-mer-2 substrate, binding of the oligosaccharide within the cleft is nearly identical between the two 8-mers (Figure 4A). In the case of 8-mer-1, there is clear density in the channel for five saccharides (-GlcNS6S-GlcA-GlcNS6S-GlcA-GlcNS6S-) with a mostly disordered GlcA on the reducing end of the visible density (Supporting Information Figure S21A). Due to the repeating disaccharide nature of 8-mer-1, the exact register of the oligosaccharides is unknown, as it is possible that additional

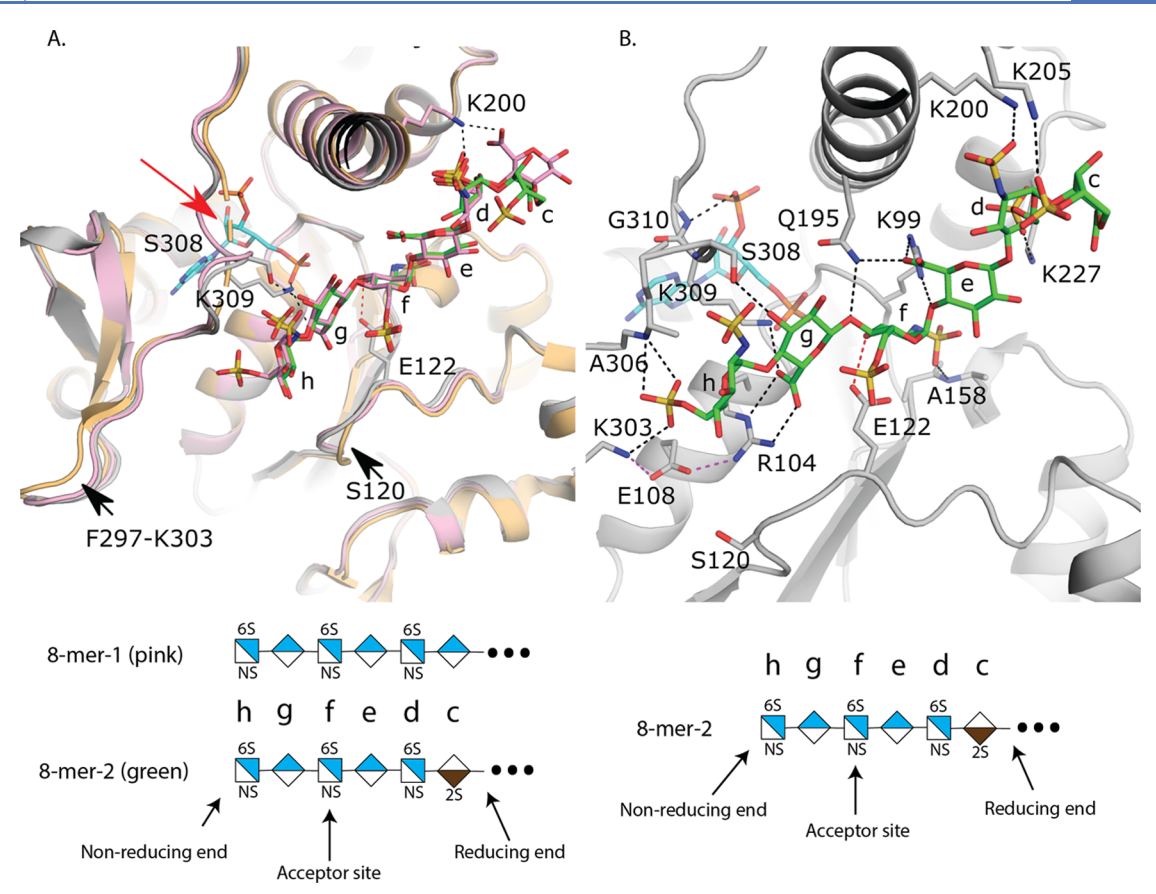


Figure 4. Crystal structures of 3-OST-5. (A) Superposition of 3-OST-5 with substrates 8-mer-1 (pink, protein light pink), 8-mer-2 (green, protein gray), and no substrate bound (protein light orange, PDBidcode: 3bd9). All structures contain PAP co-factor. PAP from the 8-mer-2 structure is shown (cyan). Loops that change positions upon binding the substrate are indicated with an arrow. The missing loop from the apo structure is represented by a dashed loop and denoted with a red arrow. (B) Interactions between substrate 8-mer-2 (green) and 3-OST-5. Probable hydrogen bonds between 8-mer-2 and 3-OST-5 are shown in dashed black lines. Interaction between Glu122 and the acceptor 3-OH group is shown as a dashed red line, and Glu108 interactions are displayed as magenta dashed lines. Saccharides are labeled c through h with shorthand structures of 8-mer-1 and -2 presented below each panel.

disordered saccharides could be present on either end of the modeled hexasaccharide. Interestingly, 8-mer-2 binds in the identical conformation as 8-mer-1, with six ordered saccharides (Figure 4A,B and Supporting Information Figure S21B). As both uronic acids present from the nonreducing end are clearly GlcA, it can be concluded that the terminal nonreducing end GlcNS6S (saccharide h) is bound in the pocket, and the IdoA2S (saccharide c) is the last ordered residue on the reducing end. Due to the high similarity in binding and the better quality of data (higher resolution and not as anisotropic) for the 8-mer-2 structure, the analysis will focus on this structure. In the 8-mer-2 substrate, the IdoA2S is modeled in the <sup>1</sup>C<sub>4</sub> chair conformation, while all other saccharides are found in the expected  ${}^4C_1$  conformation (Figure 4B). The nonreducing end GlcNS6S (saccharide h) is found extended between residues Ala306 and Ser120 at the "top" of the cleft and "bottom" of the cleft, respectively. These residues have been speculated to participate in the specificity of the 3-OST isoforms by regulating the trajectories of the substrates through the cleft, based on the sugar conformation of the saccharide at position g.25 In addition, the 6-O-sulfo group forms interactions with the side chain from Lys303 and a backbone hydrogen bond with the amide nitrogen from Ala306. GlcA saccharide g is involved in a bidentate interaction between the carboxylate and the guanidinium group of Arg104 that lies

beneath saccharide h in the cleft. The 3-OH of saccharide g forms a hydrogen bond with Ser308, helping to order this previously disordered loop. The acceptor GlcNS6S (saccharide f) is found at the active site, with the 3-OH acceptor within hydrogen-bonding distance to the proposed catalytic base, Glu122, and 5.5 Å from the phosphorous atom of the 5'phosphate of the leaving group product PAP, consistent with a catalytically relevant position, based on the proposed in-line transfer catalytic mechanism. <sup>20,27</sup> Also contributing to binding is the NS moiety that forms a hydrogen bond with a backbone amide from Ala158. There are fewer interactions with the substrate on the reducing side of saccharide f. GlcA (saccharide e) forms interactions with Gln195 and Arg99 via interactions with the carboxylate, while the NS group of GlcNS6S at position d forms an interaction with Arg200 and a possible interaction between the 6S group and Lys227. IdoA2S (saccharide c) has the weakest density of all of the saccharides, with only a single interaction between the 2-O-sulfo group and Lys205. In the case of 8-mer-1, the GlcA at position c forms a potential interaction with Lys200 via its carboxylate group (Figure 4A).

Structurally Guided Mutations of 3-OST-5 Resulted in Changes to Substrate Specificity. Amino acid residues near the substrate binding cleft were selected for site-directed mutagenesis to evaluate their roles in regulating substrate

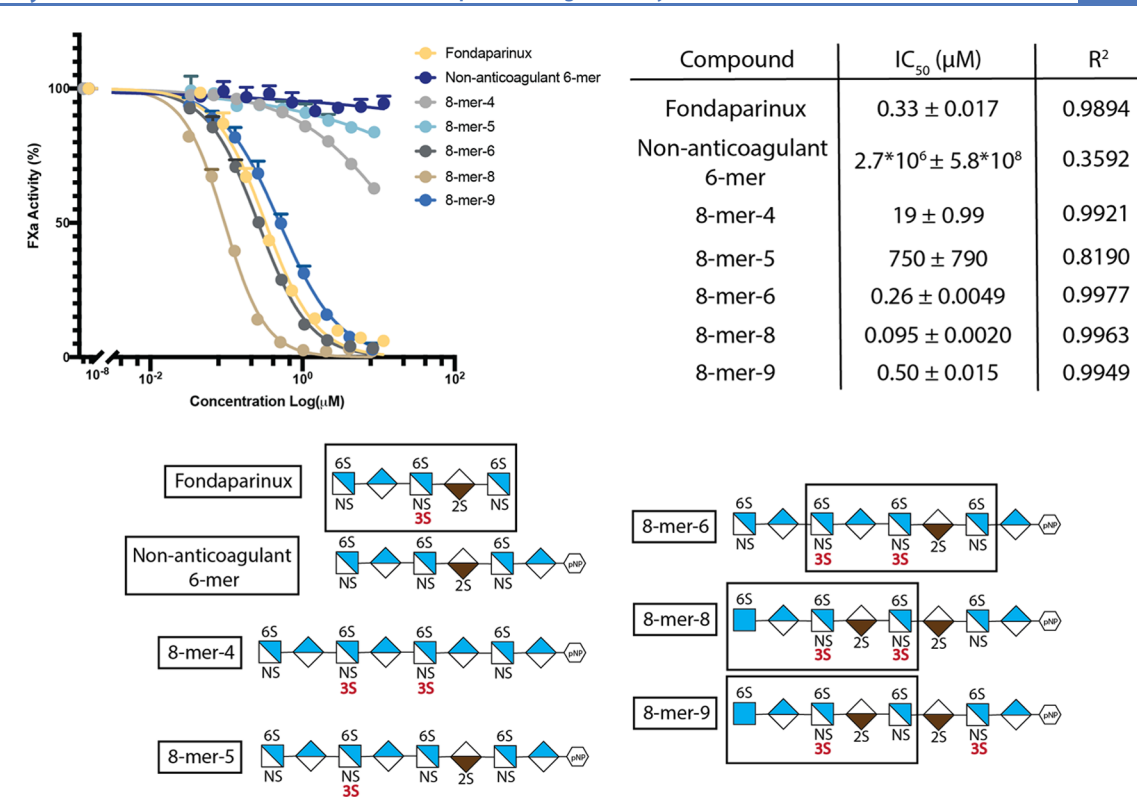


Figure 5. 3-OST-5 products have varying anti-FXa activities. 8-mer products of 3-OST-5 were assessed for anti-FXa activity in a standard chromogenic assay. Fondaparinux and a non-anticoagulant 6-mer lacking 3-O-sulfation were used as positive and negative controls, respectively. The antithrombin (AT) pentasaccharide binding sequence in 8-mers 6, 8, and 9 is boxed. These three 8-mers display strong anti-FXa activity. 8-mers 4 and 5 had minimal anti-FXa activity, consistent with their lack of the AT-binding pentasaccharide. Shorthand structures for 8-mers and non-anticoagulant 6-mer used in the analysis are shown at the bottom of the figure.

selectivity. The mutants were generated and screened against three oligosaccharides, including 8-mer-1, -2, and -3, in an HPLC assay (Supporting Information Table S2). While most mutants showed a modest effect on activity (25-117% wt activity), the E108R mutant displayed a 95% decrease in enzymatic activity against all three 8-mer substrates. This suggests that the negatively charged amino acid side chain from Glu108 residue plays an essential role for substrate recognition/binding, potentially by helping to organize the nonreducing end of the binding pocket through hydrogen bonding with Arg104 and Lys303 (Figure 4B). The mutation of A306H converts the alanine at this position to a histidine that is found in 3-OST-1. This mutation was previously shown to give 3-OST-5 more 3-OST-1-like activity on heterogeneous substrates and was suggested to function as a substrate "gate", although the composition of the substrate was not analyzed.<sup>25</sup> To better understand how this mutation might affect the specificity within the active site, we analyzed the products produced using the three substrates 8-mer-1, -2, and -3. The A306H mutant showed different degrees of change in products produced from those three 8-mer substrates (Supporting Information Figure S22). No difference between the A306H mutant and wild-type enzyme was observed when 8-mer-1 was used as a substrate. A small difference was observed in generating 8-mer-6 when 8-mer-2 was the substrate. An obvious decrease in generating di-3-O-sulfated products (or 8mer-8 and 8-mer-9) was observed when 8-mer-3 was the substrate. The A306H mutant, unlike wild-type enzyme, only produced 8-mer-7, a mono-3-O-sulfated product (Supporting Information Figure S22). The lack of 8-mer-8 and 8-mer-9

products for A306H mutant raise the possibility that the A306 residue confers the ability to generate the disaccharide domain of -IdoA2S-GlcNS3S6S-. This is consistent with the postulated role of the histidine at the "gate" in 3-OST-1 in selecting for -GlcA-GlcNS6S- containing substrates.<sup>25</sup>

3-OST-5 Generates 8-mer Products with Varying Degrees of the Anti-Factor Xa (FXa) Activity. To assess the biological implications of 3-OST-5-modified HS, 8-mer products were analyzed for anticoagulant activity, as measured by the anti-factor Xa (FXa) assay (Figure 5). We discovered that 8-mer products display a spectrum of anticoagulant activity, from very weak to very strong, depending on the saccharide sequences. The IC<sub>50</sub> value of 8-mer-8 was ~5-fold lower than that of 8-mer-6 and -9, suggesting that 8-mer-8 has the strongest anticoagulant activity. Comparing the saccharide sequences of 8-mer-6, 8-mer-8 and 8-mer-9, a difference in the relative location of the two 3-O-sulfated glucosamine (GlcNS3S6S) saccharides exists. In 8-mer-8, the two GlcNS3S6S saccharides are separated by an IdoA2S, whereas in 8-mer-6, the two GlcNS3S6S saccharides are separated by a GlcA. In 8-mer-9, the two GlcNS3S6S residues are separated by three sugar units consisting of two IdoA2S saccharides and one GlcNS6S saccharide. It should be noted that 8-mer-6, -8, and -9 all contain the antithrombin (AT)-binding pentasaccharide sequence, GlcNS6S (GlcNAc6S)-GlcA-GlcNS3S6S-IdoA2S-GlcNS6S- (boxed pentasaccharide sequence in Figure 5). The relationship between the pentasaccharide sequence and anticoagulant activity was further supported by the analysis of 8-mer-4 and -5, since each had no to weak anti-FXa activity. The 8-mer-4 does not contain an IdoA2S, which is a required

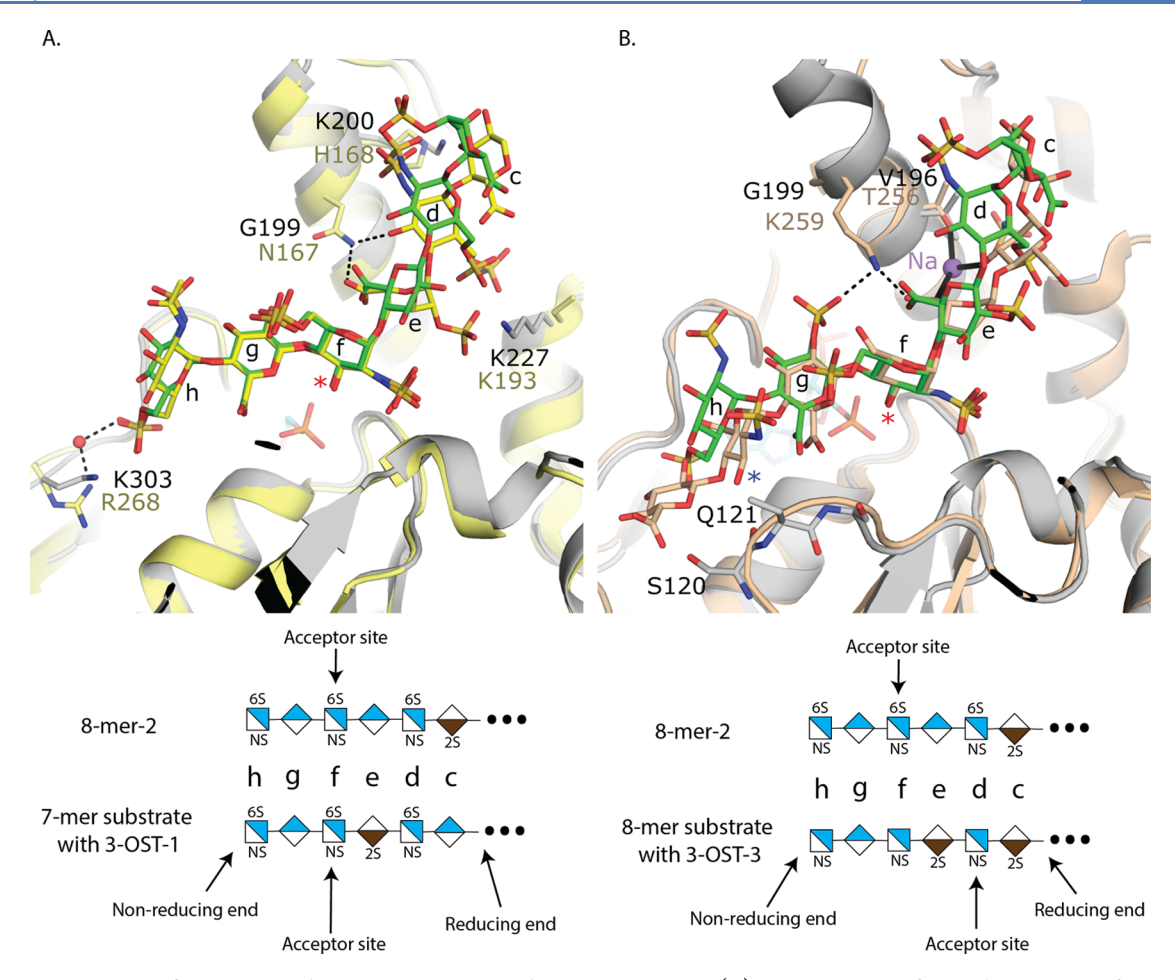


Figure 6. Superposition of 3-OST-1 and -3 onto 3-OST-5 with 8-mer-2 present. (A) Superposition of crystal structures of 3-OST-1 with heptasaccharide bound (yellow, protein light yellow; PDBidcode 3uan) onto 3-OST-5 with 8-mer-2 bound (protein in gray, 8-mer-2 in green). (B) Superposition of ternary complex crystal structures of 3-OST-3 with PAP (cyan) and the octasaccharide substrate (3-OST-3 in wheat for both protein and substrate PDB code 6xl8; 3-OST-5 protein in gray and 8-mer-2 in green). The acceptor 3-OH is marked with a red asterisk, while the 3-OH on 3-OST-3 saccharide h is marked with a blue asterisk. Saccharides are labeled c—h, and the Na ion bound to 3-OST-3 is shown as a purple sphere, with chelating interactions shown in solid black lines. Select hydrogen bonds between 3-OST-1 and 3-OST-3 with their substrates are shown in black dashed lines. Shorthand structures for the oligosaccharide substrate in each crystal structure are presented below each panel.

saccharide unit for displaying anticoagulant activity. <sup>28</sup> 8-mer-5 lacks anticoagulant activity because a GlcA saccharide, rather than an IdoA2S saccharide, is located on the reducing end of the GlcNS3S6S. It is known that an IdoA2S or an IdoA saccharide is required to be present at the reducing end of the GlcNS3S6S saccharide, in the context of -GlcNS3S6S-IdoA2S-or -GlcNS3S6S-IdoA-, to display anticoagulant activity. <sup>29</sup>

# DISCUSSION

The 3-OSTs are a unique family of HS biosynthetic enzymes. These enzymes transfer a sulfo group to synthesize 3-O-sulfated HS polysaccharides associated with widely variable biological functions.<sup>30</sup> The substrate selectivity among different isoforms of 3-OSTs can be distinguished experimentally.<sup>31</sup> Understanding the substrate recognition mechanism offers insights into how the biosynthesis of HS is regulated within cells. Recently, chemoenzymatic synthesis of structurally homogeneous HS oligosaccharides has been developed.<sup>2</sup> An in-depth understanding of the substrate specificity of new 3-OST isoforms permits the use of these new enzymes for the synthesis of 3-O-sulfated oligosaccharides for biological studies and the development of HS-based therapeutics.<sup>32</sup> In this manuscript, we employed a series of HS octasaccharides to

carry out the crystal structural analysis of 3-OST-5. For the first time, we solved the structures of 3-OST-5 in complex with oligosaccharide substrates. Comparing the crystal structures of 3-OST isoforms 1, 3, and 5 with substrate bound, <sup>19,21</sup> we found that the active sites are very similar, although subtle structural differences exist. To our surprise, we discovered that the presence of IdoA2S reduces the reactivity of 3-OST-5 for modification. Results from extensive structural comparison and homology analysis among 3-OST-1, 3-OST-3, and 3-OST-5 suggest that multiple factors contribute to the substrate specificity.

3-OST-5 and 3-OST-1 both require substrates carrying 6-O-sulfation, based on the enzyme activity measurements. The requirement for 6-O-sulfated substrate is supported by the crystal structures, which reveal interactions of the 6-O-sulfo groups on saccharide h with Lys303 and possibly saccharide d of the 8-mer-2 substrate with Lys227 (Figure 4B). The GlcNS6S at saccharide h superimposes well with that of 3-OST-1 substrate (Figure 6A). The 3-OST-1 mutant R268A reduced the activity to 7% of wild type enzyme, supporting its role in 6-O-sulfo group binding. While the positions of the 6-O-sulfo group at saccharide d for the 3-OST-1 and 3-OST-5 substrates differ in crystal structures, Lys193 of 3-OST-1,

equivalent to Lys227 of 3-OST-5, is mostly disordered and does not appear to participate in the substrate binding. Interestingly, there are no interactions with the 6-O-sulfo group of the acceptor GlcNS6S saccharide f for either 3-OST-1 or 3-OST-5. The observation suggests that both 3-OST-5 and 3-OST-1 might be able to react with oligosaccharides that are partially 6-O-sulfated. Indeed, we demonstrated that 3-OST-1 sulfates partially 6-O-sulfated oligosaccharide substrates.<sup>33</sup>

3-OST-5 enzyme displays preferences to the saccharides around the acceptor site with the following order: (1) flanking GlcA on both sides of the acceptor, (2) GlcA on the nonreducing side and IdoA2S on the reducing side, (3) IdoA2S on the nonreducing side and GlcA on the reducing side, and (4) least preferred flanking IdoA2S on both sides of acceptor. The crystal structures also provide insight into the uronic acid saccharide preference of GlcA for both saccharides flanking the acceptor GlcNS6S. Despite being given a substrate (8-mer-2) that would allow for 3-OST-5 to engage in three different ways, 3-OST-5 crystallized with GlcA flanking the acceptor GlcNS6S saccharide at saccharides g and e (Figure 4B). This is consistent with a preference for flanking GlcA saccharides to the acceptor GlcNS6S. Superpositions of the crystal structure of 3-OST-5 with 8-mer-2 bound with 3-OST-3 with the preferred two IdoA2S saccharides flanking the acceptor glucosamine reveal that the acceptor glucosamines superimpose well and are in identical conformations (Figure

The conformational flexibility of the IdoA2S saccharide could play a role in substrate recognition. In 3-OST-3, both IdoA2S saccharides are in the skew boat  $({}^{2}S_{0})$  conformation. This places the carboxylate on the IdoA2S at saccharide e within 3.7 Å of the 2-O-sulfo group on the IdoA2S at saccharide g. This accumulation of negative charge is partially alleviated by Lys259 for 3-OST-3, which hydrogen-bonds with both groups (Figure 6B).31 Gly199 sits at the equivalent site in 3-OST-5 and is unable to form these interactions, resulting in a potential charge repulsion if IdoA2S was present at saccharide g. This would also place the 2-O-sulfo group within 4 Å of the N-sulfo group on the glucosamine at saccharide h. Finally, the <sup>2</sup>S<sub>0</sub> conformation results in a different position of the nonreducing end of the saccharide, which alters the trajectory of the substrate through the space between Ala306 and Ser120 in 3-OST-5, known as the gate structure. 25 This could affect the protein interactions with the 6-O-sulfo and the N-sulfo on saccharide h. While the substrates for both 3-OST-1 and 3-OST-3 have IdoA2S on the reducing side of the acceptor, they are in different conformations. Based on crystal structures, 3-OST-3 interacts with the IdoA2S in the  ${}^2S_0$  conformation via an interaction with a bridging sodium ion that also interacts with Thr256 (Figure 6B). 3-OST-1 and 3-OST-5 contain a Val at this position (Val164 and Val196, respectively) that would preclude coordinating a sodium ion at this position. The IdoA2S on the reducing side of the acceptor for 3-OST-1 is in the <sup>1</sup>C<sub>4</sub> conformation (Figure 6A). Asn167 of 3-OST-1 (equivalent to Gly199 in 3-OST-5), forms interactions with both the carboxylate of the 2-O-sulfo group of IdoA2S at saccharide e and the 3-OH position of the GlcNS6S at saccharide d for 3-OST-1 (Figure 6A). This may help maximize the binding potential of a <sup>1</sup>C<sub>4</sub> conformation at this position. In addition, a His168 in 3-OST-1 is situated near the 2-O-sulfo from saccharide d. A H168A mutation reduced the activity of 3-OST-1 by 50%, suggesting that it contributes to substrate binding. 19 In 3-OST-5, the equivalent residue Lys200

can extend further away from the binding pocket to interact with the N-sulfo group of the glucosamine at saccharide d due to the  ${}^4C_1$  conformation of the GlcA at saccharide e, supporting a preference for a GlcA at that saccharide. Thus, while binding of an IdoA2S on the nonreducing side could introduce charge repulsion in addition to disrupting interactions with the substrate, placement of an IdoA2S on the reducing side could simply reduce favorable interactions. The preference of 3-OST-5 to produce more of 8-mer-9 than 8mer-8, in addition to product inhibition, could be due to two possible structurally based reasons; (1) having two flanking IdoA2S has the deleterious additive effects of the individual IdoA2Ss being present and/or (2) a 3-O-Sulfo group at saccharide h when there is a IdoA2S at saccharide e would result in clashes with residues Ser120 and Gln121, based on the position of the substrate orientation in 3-OST-3 (Figure 6B).

The results of these studies provide a starting point for understanding the specificity of 3-OST-5 utilizing smaller, 8-mer oligosaccharides. While the biological substrates of the enzyme are known to be much longer polysaccharides, current oligosaccharide sequencing methods limit our ability to conduct specificity studies using these longer structures. It is interesting to note that the 8-mers extend across most of the substrate binding cleft, suggesting that the critical elements for binding are accounted for by these substrates in the crystal structures. Additional studies of the sequence/structure around modification sites on polysaccharides are of interest but would require more sophisticated sequencing methods. Such studies could reveal whether the observed specificity reported here is also observed *in vivo*.

An interesting finding from our study is that 3-OST-5 generates both anticoagulant and non-anticoagulant oligosaccharides, opening a new avenue for developing HS-based therapeutics. These oligosaccharides are all highly sulfated and show the same levels of sulfo groups per disaccharide unit. It was widely expected that fully sulfated HS oligosaccharides carrying 3-O-sulfation would display anticoagulant activity. The results from our studies suggest that 3-OST-5 can generate non-anticoagulant 3-O-sulfated 8-mers, i.e., 8-mer-4 and 8-mer-5. The synthesis of anticoagulant and nonanticoagulant 8-mers can be achieved by controlling the number and position of IdoA2S saccharide in the substrates subjected to 3-OST-5 modification. These non-anticoagulant 3-O-sulfated oligosaccharides could be used to target proteins in alternate pathways, such as inflammation, without the risk of bleeding side effects.

# ASSOCIATED CONTENT

### Supporting Information

The Supporting Information is available free of charge at https://pubs.acs.org/doi/10.1021/acscatal.1c04520.

Experimental procedures, supplementary tables, and supplementary figures are included (PDF)

## AUTHOR INFORMATION

# **Corresponding Author**

Jian Liu – Division of Chemical Biology and Medicinal Chemistry, Eshelman School of Pharmacy, University of North Carolina, Chapel Hill, North Carolina 27599, United States; ⊚ orcid.org/0000-0001-8552-1400; Email: jian liu@unc.edu

### **Authors**

- Rylee Wander Division of Chemical Biology and Medicinal Chemistry, Eshelman School of Pharmacy, University of North Carolina, Chapel Hill, North Carolina 27599, United States
- Andrea M. Kaminski Genome Integrity and Structural Biology Laboratory, National Institute of Environmental Health Sciences, National Institutes of Health, Research Triangle Park, North Carolina 27711, United States
- **Zhangjie Wang** Division of Chemical Biology and Medicinal Chemistry, Eshelman School of Pharmacy, University of North Carolina, Chapel Hill, North Carolina 27599, United States
- Eduardo Stancanelli Division of Chemical Biology and Medicinal Chemistry, Eshelman School of Pharmacy, University of North Carolina, Chapel Hill, North Carolina 27599, United States
- Yongmei Xu Division of Chemical Biology and Medicinal Chemistry, Eshelman School of Pharmacy, University of North Carolina, Chapel Hill, North Carolina 27599, United States
- Vijayakanth Pagadala Glycan Therapeutics Corp, Raleigh, North Carolina 27606, United States
- Jine Li Division of Chemical Biology and Medicinal Chemistry, Eshelman School of Pharmacy, University of North Carolina, Chapel Hill, North Carolina 27599, United States
- Juno M. Krahn Genome Integrity and Structural Biology Laboratory, National Institute of Environmental Health Sciences, National Institutes of Health, Research Triangle Park, North Carolina 27711, United States
- Truong Quang Pham Glycan Therapeutics Corp, Raleigh, North Carolina 27606, United States
- Lars C. Pedersen Genome Integrity and Structural Biology Laboratory, National Institute of Environmental Health Sciences, National Institutes of Health, Research Triangle Park, North Carolina 27711, United States

Complete contact information is available at: https://pubs.acs.org/10.1021/acscatal.1c04520

### **Author Contributions**

R.W. analyzed the substrate specificity of 3-OST-5, synthesized 8-mers, measured the anticoagulant activity of 8-mers, and wrote the manuscript. A.M.K. conducted the crystal structural trials and prepared different 3-OST-5 mutants. Z.W. assisted in the structural analysis of 8-mers using the LC-MS/MS method. E.S. conducted the NMR analysis of 8-mer-4. J.L. generated the 3-OST-5-flag tagged expression construct. J.M.K. provided technical expertise in the refinement and parameterization of oligosaccharides. T.Q.P. produced the enzymes to support the synthesis of 8-mers. L.C.P. and J.L. designed the study and wrote the manuscript. All authors contributed to manuscript writing and approved the manuscript.

## Notes

The authors declare the following competing financial interest(s): Y.X. and Jian Liu are founders of Glycan Therapeutics and have equity. V.P. is an employee of Glycan Therapeutics. T.P. is an employee of Glycan Therapeutics. Dr. Jian Liu's lab at UNC has received a gift from Glycan Therapeutics to support research in glycoscience. R.W., A.M.K., Z.W., E.S., Jine Li, J.M.K. and L.C.P. declare no competing interest.

# ■ ACKNOWLEDGMENTS

The authors thank G. Mueller and P. Tumbale for critical reading of the manuscript. This work was supported in part by the Division of Intramural Research of the National Institute of Environmental Health Sciences, National Institutes of Health Grants 1ZIA ES102645 (to L.C.P.) and by the National Institutes of Health Grants HL094463, HL144970, GM128484, GM134738, and HL139197. This work was also supported by GlycoMIP, a National Science Foundation Materials Innovation Platform funded through Cooperative Agreement DMR-1933525. Use of the Advanced Photon Source was supported by the US Department of Energy, Office of Science, Office of Basic Energy Sciences [W-31-109-Eng-38].

# REFERENCES

- (1) Bishop, J.; Schuksz, M.; Esko, J. D. Heparan sulphate proteoglycans fine-tune mammalian physiology. *Nature* **2007**, 446, 1030–1037.
- (2) Liu, J.; Linhardt, R. J. Chemoenzymatic synthesis of heparan sulfate and heparin. *Nat. Prod. Rep.* **2014**, *31*, 1676–1685.
- (3) Clausen, T. M.; Sandoval, D. R.; Spliid, C. B.; Pihl, J.; Perrett, H. R.; Painter, C. D.; Narayanan, A.; Majowicz, S. A.; Kwong, E. M.; McVicar, R. N.; Thacker, B. E.; Glass, C. A.; Yang, Z.; Torres, J. L.; Golden, G. J.; Bartels, P. L.; Porell, R. N.; Garretson, A. F.; Laubach, L.; Feldman, J.; Yin, X.; Pu, Y.; Hauser, B. M.; Caradonna, T. M.; Kellman, B. P.; Martino, C.; M Gordts, P. L. S. M.; Chanda, S. K.; Schmidt, A. G.; Godula, K.; Leibel, S. L.; Jose, J.; Corbett, K. D.; Ward, A. B.; Carlin, A. F.; Esko, J. D. SARS-CoV-2 Infection Depends on Cellular Heparan Sulfate and ACE2. *Cell* 2020, 183, 1043–1057. (4) Gama, C.; Tully, S. E.; Sotogaku, N.; Clark, P. M.; Rawat, M.;
- (4) Gama, C.; Tully, S. E.; Sotogaku, N.; Clark, P. M.; Rawat, M.; Vaidehi, N.; Goddard, W. A.; Nishi, A.; Hsieh-Wilson, L. C. Sulfation patterns of glycosaminoglycans encode molecular recognition and activity. *Nat. Chem. Biol.* **2006**, *2*, 467–473.
- (5) Esko, J. D.; Lindahl, U. Molecular diversity of heparan sulfate. J. Clin. Invest. 2001, 108, 169–173.
- (6) Xu, Y.; Masuko, S.; Takieddin, M.; Xu, H.; Liu, R.; Jing, J.; Mousa, S. A.; Linhardt, R. J.; Liu, J. Chemoenzymatic synthesis of homogeneous ultra-low molecular weight heparin. *Science* **2011**, 334, 498–501.
- (7) Xu, Y.; Cai, C.; Chandarajoti, K.; Hsieh, P.; Lin, Y.; Pham, T. Q.; Sparkenbaugh, E. M.; Sheng, J.; Key, N. S.; Pawlinski, R. L.; Harris, E. N.; Linhardt, R. J.; Liu, J. Homogeneous and reversible low-molecular weight heparins with reversible anticoagulant activity. *Nat. Chem. Biol.* **2014**, *10*, 248–250.
- (8) Wang, Z.; Arnold, K.; Dhurandhare, V. M.; Xu, Y.; Liu, J. Investigation of the biological functions of heparan sulfate using a chemoenzymatic synthetic approach. *RSC Chem. Biol.* **2021**, *2*, 702–712.
- (9) Xu, Y.; Chandarajoti, K.; Zhang, X.; Pagadala, V.; Dou, W.; Hoppensteadt, D. M.; Sparkenbaugh, E.; Cooley, B.; Daily, S.; Key, N. S.; Severynse-Stevens, D.; Fareed, J.; Linhardt, R. J.; pawlinski, R.; Liu, J. Synthetic oligosaccharides can replace animal-sourced low-molecular weight heparins. *Sci. Transl. Med.* **2017**, *9*, No. eaan5954.
- (10) Shworak, N. W.; Liu, J.; Petros, L. M.; Zhang, L.; Kobayashi, M.; Copeland, N. G.; Jenkins, N. A.; Rosenberg, R. D. Diversity of the extensive heparan sulfate D-glucosaminyl 3-O-sulfotransferase (3-OST) multigene family. *J. Biol. Chem.* **1999**, 274, 5170–5184.
- (11) Shukla, D.; Liu, J.; Blaiklock, P.; Shworak, N. W.; Bai, X.; Esko, J. D.; Cohen, G. H.; Eisenberg, R. J.; Rosenberg, R. D.; Spear, P. G. A novel role for 3-O-sulfated heparan sulfate in herpes simplex virus 1 entry. *Cell* **1999**, *99*, 13–22.
- (12) Li, J.; Su, G.; Xu, Y.; Arnold, K.; Pagadala, V.; Wang, C.; Liu, J. Synthesis of 3-O-Sulfated Heparan Sulfate Oligosaccharides Using 3-O-Sulfotransferase Isoform 4. ACS Chem. Biol. 2021, 16, 2026–2035. (13) Thacker, B. E.; Seamen, E.; Lawrence, R.; Parker, M. W.; Xu,

Y.; Liu, J.; Vander, K. C. W.; Esko, J. D. Expanding the 3-O-Sulfate

- Proteome-Enhanced Binding of Neuropilin-1 to 3-O-Sulfated Heparan Sulfate Modulates Its Activity. ACS Chem. Biol. 2016, 11, 971–980.
- (14) Patel, V. N.; Lombaert, I. M. A.; Cowherd, S. N.; Shworak, N.; Xu, Y.; Liu, J.; Hoffman, M. P. 3-O-sulfated heparan sulfate controls epithelial Kit+FGFR2b+ progenitor expansion via rapid autocrine regulation of 3-O-sulfotransferases. *Dev. Cell* **2014**, *29*, 662–673.
- (15) de Agostini, A. I.; Dong, J. C.; de Vantery Arrighi, C.; Ramus, M. A.; Dentand-Quadri, I.; Thalmann, S.; Ventura, P.; Ibecheole, V.; Monge, F.; Fischer, A. M.; HajMohammadi, S.; Shworak, N. W.; Zhang, L.; Zhang, Z.; Linhardt, R. J. Human follicular fluid heparan sulfate contains abundant 3-O-sulfated chains with anticoagulant activity. *J. Biol. Chem.* **2008**, 283, 28115–28124.
- (16) Denys, A.; Allain, F. The Emerging Roles of Heparan Sulfate 3-O-Sulfotransferases in Cancer. *Front, Oncol,* **2019**, *9*, No. 507.
- (17) Sepulveda-Diaz, J. E.; Alavi Naini, S. M.; Huynh, M. B.; Ouidja, M. O.; Yanicostas, C.; Chantepie, S.; Villares, J.; Lamari, F.; Jospin, E.; van Kuppevelt, T. H.; Mensah-Nyagan, A. G.; Raisman-Vozari, R.; Soussi-Yanicostas, N.; Papy-Garcia, D. HS3ST2 expression is critical for the abnormal phosphorylation of tau in Alzheimer's disease-related tau pathology. *Brain* **2015**, *138*, 1339–1354.
- (18) Zhao, J.; Zhu, Y.; Song, X.; Xiao, Y.; Su, G.; Liu, X.; Wang, Z.; Xu, Y.; Liu, J.; Eliezer, D.; Ramlall, T. E.; Lippens, G.; Gibson, J.; Zhang, F.; Linhardt, R. J.; Wang, L.; Wang, C. 3-O-sulfation of heparan sulfate enhances tau interaction and cellular uptake. *Angew. Chem., Int. Ed.* **2020**, *59*, 1818–1827.
- (19) Moon, A. F.; Xu, Y.; Woody, S.; Krahn, J. M.; Linhardt, R. J.; Liu, J.; Pedersen, L. C. Dissecting substrate recognition mode of heparan sulfate 3-O-sulfotransferases for the biosynthesis of anticoagulant heparin. *Proc. Natl. Acad. Sci. U.S.A.* **2012**, *109*, 5256–5270.
- (20) Moon, A.; Edavettal, S. C.; Krahn, J. X.; Munoz, E. M.; Negishi, M.; Linhardt, R. J.; Liu, J.; Pedersen, L. C. Structural analysis of the sulfotransferase (3-OST-3) involved in the biosynthesis of an entry receptor of herpes simplex virus 1. *J. Biol. Chem.* **2004**, 279, 45185–45193
- (21) Wander, R.; Kaminski, A. M.; Xu, Y.; Pagadala, V.; Krahn, J. M.; Pham, T. Q.; Liu, J.; Pedersen, L. C. Deciphering the substrate recognition mechanisms of the heparan sulfate 3-O-sulfotransferase-3. *RSC Chem. Biol.* **2021**, *2*, 1239–1248.
- (22) Dhurandhare, V. M.; Pagadala, V.; Ferreira, A.; Muynck, L. D.; Liu, J. Synthesis of 3-O-sulfated disaccharide and tetrasaccharide standards for compositional analysis of heparan sulfate. *Biochemistry* **2020**, *59*, 3186–3192.
- (23) Venkataraman, G.; Shriver, Z.; Raman, R.; Sasisekharan, R. Sequencing complex polysaccharides. *Science* **1999**, *286*, 537–542.
- (24) Wang, Z.; Hsieh, P.-H.; Xu, Y.; Thieker, D.; Chai, E. J. E.; Xie, S.; Cooley, B.; Woods, R. J.; Chi, L.; Liu, J. Synthesis of 3-O-sulfated oligosaccharides to understand the relationship between structures and functions of heparan sulfate. *J. Am. Chem. Soc.* **2017**, *139*, 5249–5256.
- (25) Xu, D.; Moon, A.; Song, D.; Pedersen, L. C.; Liu, J. Engineering sulfotransferases to modify heparan sulfate. *Nat. Chem. Biol.* **2008**, *4*, 200–202.
- (26) Edavettal, S. C.; Lee, K. A.; Negishi, M.; Linhardt, R. J.; Liu, J.; Pedersen, L. C. Crystal structure and mutational analysis of heparan sulfate 3-O-sulfotransferase isoform 1. *J. Biol. Chem.* **2004**, 279, 25789—25797.
- (27) Kakuta, Y.; Li, L.; Pedersen, L. C.; Pedersen, L. G.; Negishi, M. Heparan sulphate N-sulphotransferase activity: reaction mechanism and substrate recognition. *Biochem. Soc. Trans.* **2003**, *31*, 331–334.
- (28) Das, S.; Mallet, J.; Esnault, J.; Driguez, P.; Duchaussoy, P.; Sizun, P.; Herault, J.; Herbert, J.; Petitou, M.; Sinaÿ, P. Synthesis of conformationally locked L-iduronic acid derivatives: direct evidence for a critical role of the skew-boat 2S0 conformer in the activation of antithrombin by heparin. *Chemistry* **2001**, *7*, 4821–4834.
- (29) Hsieh, P.-H.; Thieker, D. F.; Guerrini, M.; Woods, R. J.; Liu, J. Uncovering the relationship between sulphation patterns and

- conformation of iduronic acid in heparan sulphate. Sci. Rep. 2016, 6, No. 29602.
- (30) Thacker, B.; Xu, D.; Lawrence, R.; Esko, J. Heparan sulfate 3-O-sulfation: a rare modification in search of a function. *Matrix Biol.* **2014**, *35*, 60–72.
- (31) Liu, J.; Moon, A. F.; Sheng, J.; Pedersen, L. C. Understanding the substrate specificity of the heparan sulfate sulfotransferases by a combined synthetic crystallographic approach. *Curr. Opin. Struct. Biol.* **2012**, *22*, 550–557.
- (32) Arnold, K.; Liao, Y.-E.; Liu, J. Potential use of antiinflammatory synthetic heparan sulfate to attenuate liver damage. *Biomedicines* **2020**, *8*, No. 503.
- (33) Yi, L.; Xu, Y.; Kaminski, A. M.; Chang, X.; Pagadala, V.; Horton, M.; Su, G.; Wang, Z.; Lu, G.; Conley, P.; Zhang, Z.; Pedersen, L. C.; Liu, J. Using enigneered 6-O-sulfotransferase to improve the synthesis of anticoagulant heparin. *Org. Biomol. Chem.* **2020**, *18*, 8094–8102.